

Superconducting Thin Film Nanostructures as Terahertz and Infrared Heterodyne and Direct Detectors

Gregory Goltsman^{1,2*}

¹Moscow State Pedagogical University, 119991 Moscow, Russia,

² Zavoisky Physical-Technical Institute of the Russian Academy of Sciences, 420029 Kazan, Russia

* e-mail: goltsman10@mail.ru

Abstract— We present our recent achievements in the development of superconducting nanowire single-photon detectors (SNSPDs) integrated with optical waveguides on a chip. We demonstrate both single-photon counting with up to 90% on-chip-quantum-efficiency (OCDE), and the heterodyne mixing with a close to the quantum limit sensitivity at the telecommunication wavelength using single device.

Keywords—*photon counters; optical waveguides; coherent detection; optical integrated circuits; superconducting devices*

I. INTRODUCTION

During last twenty years, a new generation of superconducting detectors based on hot-electron-phenomena was developed. These sensors have already demonstrated performance that makes them devices-of-choice for many terahertz, infrared and optical applications. To date, due to the growing interest, the market for superconducting devices is gradually expanding, as evidenced by the emergence of small companies engaged in the development, improvement and commercialization of superconducting devices.

One such device is the superconducting nanowire single-photon detector (SNSPD or SSPD) [1]. SNSPDs combine high detection efficiency, low dark count rate, and high temporal resolution in a single device in visible and near IR range [2,3]. SNSPDs have been successfully employed for classical and quantum optics applications ranging from optical time domain reflectometry (OTDR), light detection and ranging (LiDAR), space-to-ground communications, quantum dot photonics, quantum key distribution to experiments with indistinguishable and entangled photon pairs and applications in the life sciences.

Further development of SSPDs can be associated with the implementation of complex integrated photonic (PICs) and quantum photonic integrated circuits (QPICs) on a single chip. Integrated circuits are resistant to mechanical vibrations and temperature fluctuations, they do not require long alignment procedure and can be easily scaled [4, 5]. To date, integrated SNSPDs have been implemented on various material platforms [6], such as silicon on insulator (SOI), gallium arsenide (GaAs), silicon nitride (Si₃N₄) and polycrystalline diamond. Each platform has its advantages and disadvantages, so further development takes place in parallel. Despite the fact that all the building blocks for a fully-functional QPIC, including single-photon sources, detectors and passive circuits, have been

demonstrated, full integration of all the components on a single chip is still a somewhat challenging and complicated task.

Recently, a fully integrated circuit including a single photon source (carbon nanotube), detectors (SNSPDs) and Si₃N₄ waveguides has already been implemented on a chip [7]. Going beyond such proof-of-principle concepts, the realization of large scale QPICs is expected to have profound impact on science and technology, material engineering, as well as quantum information processing including quantum computing, simulation and metrology.

Implementation of the travelling wave geometry allows achieving high on-chip detection efficiency (OCDE), small detector footprint, high temporal resolution, and high counting rate. However, the SNSPD being the threshold detector is not directly capable of disclosing the energy of the incident radiation.

Integration of the SNSPDs with array waveguide gratings (AWGs), acting as a demultiplexer, has been demonstrated recently [8]. Two types of devices operating near 740 nm and 1550 nm wavelengths have shown promising results, including detection efficiency and high time resolution. Demonstrated integrated circuit was successfully used to measure the emission spectrum of diamond nanocluster with embedded silicon vacancies (SiV), as well as mapped out fluorescence decay times within the cluster area simultaneously. However, all of similar approaches offer only a small number of spectral channels, which results either in limited resolution or in a narrow spectral range. Potential of fiber coupled SNSPDs for coherent detection with high wavelength resolution was demonstrated in [9]. However, use of fiber-coupled SNSPDs requires special care of the light coupling optimization (e.g., implementation of resonant layers) to enhance the detection efficiency, and free-space or fiber-optics based components are widely employed for guiding the beam.

Here we continue our study on using SNSPDs for coherent detection. We demonstrate both single-photon counting with a high OCDE as well as heterodyne detection with high spectral resolution.

II. DESIGN AND FABRICATION

An ultrathin 4-nm thick NbN film was deposited on a substrate with several functional layers: Si/SiO₂/Si₃N₄ (350 μm / 2.6 μm / 0.45 μm) by reactive magnetron sputtering in an argon and nitrogen atmosphere at a substrate temperature $T_S = 800^\circ\text{C}$. We reached a maximum critical temperature $T_c = 9.5$ K for films deposited with partial pressures of argon and nitrogen

G.G. acknowledges support by Russian Science Foundation, project 16-12-00045.

of 6×10^{-3} and 2.5×10^{-4} mbar, respectively. The sheet resistance of the deposited NbN film measured at room temperature was 620 Ohms/sq. For fabrication of nanophotonic devices we used

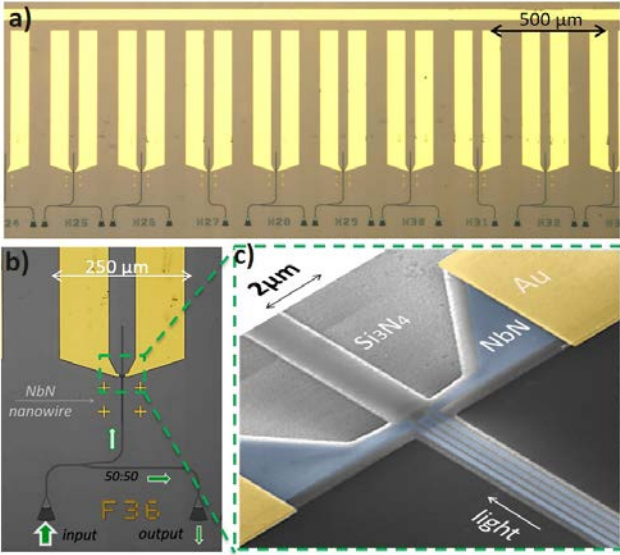


Fig. 1. Fabricated nanophotonic devices. a) Optical micrograph of the array of nanophotonic devices. b) Optical micrograph of a single nanophotonic device including Au contact pads (yellow), nanophotonic waveguide (dark gray), 50:50 Y-splitter, focusing grating couplers placed at the input and output as well as NbN nanowire, connected to Au contact pads. c) SEM image of a W-shaped NbN nanowire atop nanophotonic waveguide in false colors.

three steps of electron beam (e-beam) lithography. At the first step, using standard lift-off technique, Au-contact pads and alignment marks needed for the next steps are formed. At the second step, W-shaped NbN nanowires are formed by reactive ion etching (RIE) in CF_4 with use of the HSQ resist. Finally, nanophotonic waveguides were fabricated using negative electron maN-2403 resist and etching in atmosphere of CHF_3 .

A schematic view of a set and a single nanophotonic device are shown in Fig. 1 a,b. Such device includes two focusing grating couplers (FGC), 50:50 Y-splitter and a W-shaped NbN nanowire on top of the silicon nitride waveguide with a width of 1.3 μm . The FGCs are used for input/output light coupling to an optical single mode fiber into/out nanophotonic waveguide. The period and fill factor of FGC were optimized and provide coupling efficiency of 15% at 1550 nm wavelength at liquid helium temperatures.

III. EXPERIMENTAL SETUP

The experimental setup for demonstration of the on-chip coherent detection is shown in Fig. 2. The emitted light from tunable laser source (LS, TLS Santec 510) is divided into two equal parts by a fiber beam splitter (BS_1). The first part acts as the local oscillator (LO), while the second part, routed twice through an acousto-optic modulator (AOM, Gooch&Housego fibre Q) to relatively shift its frequency to the initial carrier frequency by a constant value of $f_{IF} = 400.016$ MHz, acts as a signal (S). LO and S are both attenuated (Att_1 , Att_2), routed through the polarization controllers (FPC_1 , FPC_2) and combined at the second fiber optics beam splitter (BS_2). A fiber array and FGCs are used to feed the light into the nanophotonic devices,

placed on a motorized stage (AttoCube System) in a cryostat at 1.7 K temperature.

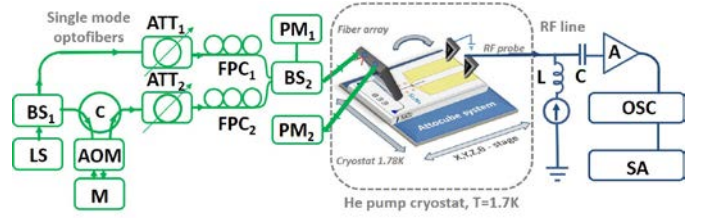


Fig. 2. Experimental setup for coherent detection using one tunable laser. Optics components are shown in green: LS-tunable laser source, BS_1 , BS_2 are 50:50 fiber beam splitters, ATT_1 , ATT_2 are tunable attenuators, C is circulator, AOM is acousto-optic modulator, M is mirror, FPC_1 , FPC_2 are fiber polarization controllers, PM_1 , PM_2 are power meters; RF components and equipment are shown in blue; L and C are inductor and capacitor forming a bias-tee, A is amplifier, OSC is oscilloscope, SA is spectrum analyzer.

The superposition of the frequency shifted EM waves mixed at the BS_2 generates a beating signal with amplitude which is risen when the two signals are in phase and canceled out when they are in anti-phase. Oscillations of the total EM field occur at the difference frequency $f_{IF} = |f_{LO} - f_S|$. The probability of detecting a photon is proportional to the instantaneous power in each time bin. For this reason the photon flux (Φ_{ph}), and therefore, the detection count rate (CR) oscillate at the same frequency f_{IF} .

IV. EXPERIMENTAL DATA

In order to find the maximum OCDE, we have made a set of nanophotonic devices with different widths of NbN superconducting nanowires on a single chip (Fig. 1a). Measurement of detection efficiency on the chip was carried out with implementation of a standard technique, the main feature of which is the precise calibration of the photon flux reaching the detector [10]. We determine OCDE as the ratio of number of the observed counts by the detector (N_c) and number of photons (N_{ph}) that reach the nanowire. The measured dependencies of the OCDE as well as dark count rate versus the normalized bias current for 60 μm W-shaped nanowire footprint and 80 nm nanowire width are shown in Fig. 3a. The dependence has the long saturation area, which theoretically indicates a good quality of the nanowire and internal detection efficiency (IDE) being close to unity. The figure shows the dependence of the OCDE on the nanowire width, measured close to the critical current $I_b = 0.95I_c$. Such dependence of OCDE versus nanowire width is connected with the influence of two factors: nanowire absorption (NA) and IDE. In general case it is the product of them: $OCDE = NA \times IDE$. The NA is associated with the value of the overlap integral waveguide evanescent mode and area of nanowire. Knowing all the geometrical parameters of nanophotonic waveguide and the nanowire, NA can be numerically calculated [11]. In Fig. 3b is shown the total NA calculated for fabricated devices using the finite element method (FEM), implemented in COMSOL multiphysics. With a large width of the nanowire (more than 80 nm), when the absorption reaches a maximum, the detection efficiency decreases, which we explain by a decrease in the IDE [12]. As the width of the nanowire decreases, its absorption also decreases, and the OCDE follows this trend. To demonstrate coherent detection, we chose a nanophotonic device with a strip width of 80 nm, which

provides the maximum OCDE. Detected beat signal by the waveguide integrated SNSPD, after amplification, was analyzed by a spectrum analyzer (SA, Ronde & Schwarz ZVL6).

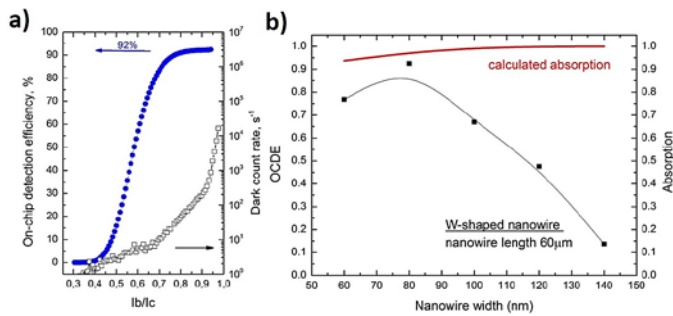


Fig. 3. a) The measured dependence of the OCDE and dark count rate versus normalized bias current for W-shaped NbN nanowire atop of Si_3N_4 rib waveguide. Maximum OCDE on a plateau 0.92. b) Measured dependence of maximum OCDE ($I_b = 0.95 I_c$) versus nanowire width for meander structured nanowire atop Si_3N_4 rib waveguide (black circles). Calculated absorption of meander structured NbN nanowires atop of Si_3N_4 rib waveguide (red line).

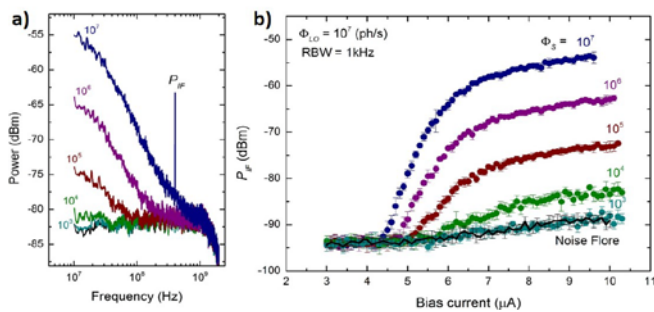


Fig. 4. a) The measured power spectral density (PSD) of signal from integrated SNSPD. PSD at photon flux from 10^3 - 10^6 measured with by LO radiation, as well as at 10^6 . b) IF power for signal and noise vs bias current.

In Fig. 4, the output signal provided by the spectrum analyzer is shown demonstrating the power spectral density (PSD) of a signal from the superconducting nanowire. The values near the curves show the value of the photon flux from the LO reaching the detector. If only one of the signals (“LO” or “S”) is present, then a trace corresponding to the power spectral density of a single pulse of the SNSPD would be seen by the SA, and there would be no beat signal at the intermediate frequency. When both the signals are present, a beat signal appears at the intermediate frequency f_{IF} . The resolution bandwidth (RBW) for these data was set to 10 kHz. The reduction of the RBW down to 1 kHz did not lead to a significant reduction in the signal and shows that the intermediate frequency is narrower than the RBW. We also measured the dependence of the signal at f_{IF} on the bias current (I_b). The P_{IF} increases with increasing I_b (Fig. 4b) and shows the similar plateau behavior as the OCDE, presented in Fig. 3a. By reducing the photon flux in the signal laser, we found that when the signal is equal to 10^3 photons per second, the peak at the intermediate frequency does not come out of the noise. The value at which the signal-to-noise ratio SNR= 1 corresponds to the photon flux ≈ 1.7 - 2×10^3 ph/s. Taking into account that the integration time $t=1/\text{RBW}$, we find that the minimum detectable

signal corresponds to about 1.8 - $2 \times h\nu$ photons into the time bin t , which approaches the quantum limit [9]. An improvement of the achieved performance as well as practical implementation should be possible in the future.

V. CONCLUSION

In conclusion, we have demonstrated the heterodyne mixing with use of the waveguide-integrated SNSPD, where the NbN superconducting nanowire is evanescently coupled to a waveguided mode field. We demonstrated both single-photon counting with up to 90% OCDE in the direct detection mode, and the heterodyne mixing with sensitivity close to the quantum limit at the telecommunication wavelength, with use of a single device.

REFERENCES

- [1] G. Gol'tsman, O. Okunev, G. Chulkova, A. Lipatov, A. Semenov, K. Smirnov, B. Voronov, A. Dzar'danov, C. Williams, R. Sobolewski, "Picosecond superconducting single-photon optical detector" *Appl. Phys. Lett.* 79 (2001): 705-707
- [2] Chandra M Natarajan, Michael G Tanner, Robert H Hadfield "Superconducting nanowire single-photon detectors: physics and applications" *Supercond. Sci. Technol.* 25 (2012) 063001
- [3] F. Najafi, F. Marsili, V. B. Verma, Q. Zhao, M. D. Shaw, K. K. Berggren, and S. Nam, "Superconducting Nanowire Architectures for Single Photon Detection," in *Superconducting Devices in Quantum Optics*, R. H. Hadfield and J. Goran, Eds. Springer, 2016, pp. 3–30.
- [4] J. W. Silverstone, D. Bonneau, J. L. O'Brien, and M. G. Thompson, "Silicon Quantum Photonics," *IEEE J. Sel. Top. Quantum Electron.*, vol. 22, no. 6, pp. 390–402, 2016.
- [5] C. P. Dietrich, A. Fiore, M. Thompson, M. Kamp, and S. Höfling, "GaAs integrated quantum photonics: Towards compact and multi-functional quantum photonic integrated circuits," *Laser Photonics Rev.*, vol. 10, pp. 1–25, 2016.
- [6] S. Bogdanov, M. Y. Shalaginov, A. Boltasseva, and V. M. Shalaev, "Material platforms for integrated quantum photonics," *Opt. Mater. Express*, vol. 7, no. 1, pp. 111–132, 2016.
- [7] S. Khasminskaya, F. Pyatkov, K. Slowik, S. Ferrari, O. Kahl, V. Kovalyuk, P. Rath, A. Vetter, F. Hennrich, M. M. Kappes, G. Gol'tsman, A. Korneev, C. Rockstuhl, R. Krupke, and W. H. P. Pernice, "Fully integrated quantum photonic circuit with an electrically driven light source," *Nat. Photonics*, vol. 10, pp. 727–733, 2016.
- [8] O. Kahl, S. Ferrari, V. Kovalyuk, A. Vetter, G. Lewes-Malandrakis, C. Nebel, A. Korneev, G. Gol'tsman, and W. Pernice, "Spectrally multiplexed single-photon detection with hybrid superconducting nanophotonic circuits," *Optica*, vol. 4, no. 5, pp. 557–562, 2017.
- [9] M. Shcherbatenko, Y. Lobanov, A. Semenov, V. Kovalyuk, A. Korneev, R. Ozhegov, A. Kazakov, B. M. Voronov, and G. N. Gol'tsman, "Potential of a Superconducting Photon Counter for Heterodyne Detection at Telecommunication Wavelength," *Opt. Express*, vol. 179, no. 1980, pp. 1178–1181, 2016.
- [10] W. H. P. Pernice, C. Schuck, O. Minaeva, M. Li, G. N. Gol'tsman, A. V. Sergienko, and H. X. Tang, "High-speed and high-efficiency travelling wave single-photon detectors embedded in nanophotonic circuits," *Nat. Commun.*, vol. 3, p. 1325, 2012.
- [11] V. Kovalyuk, W. Hartmann, O. Kahl, N. Kaurova, A. Korneev, G. Gol'tsman, and W. H. P. Pernice, "Absorption engineering of NbN nanowires deposited on silicon nitride nanophotonic circuits," *Opt. Express*, vol. 21, no. 19, pp. 22683–22692, 2013.
- [12] S. Ferrari, O. Kahl, V. Kovalyuk, G. N. Gol'tsman, A. Korneev, and W. H. P. Pernice, "Waveguide-integrated single- and multi-photon detection at telecom wavelengths using superconducting nanowires," *Appl. Phys. Lett.*, vol. 106, no. 15, p. 151101, 2015.